Memorias del XVI Congreso Latinoamericano de Control Automático, CLCA 2014
Octubre 14-17, 2014. Cancún, Quintana Roo, México

Quadripole Models for Gas Networks

Sara T. Baltazar * **Paulo Lopes dos Santos** **
T-P Azevedo Perdicoúlis ***

* *Universidade de Trás-os-Montes e Alto Douro (UTAD), 5001-801 Vila Real - Portugal (e-mail: sarabaltazar@gmail.com).*
** *Electrical Engineering Department, Faculdade de Engenharia da Universidade do Porto (FEUP), 4200-464 Porto, Portugal (e-mail: pjsantos@fe.up.pt)*
*** *ISR-Coimbra and UTAD, Portugal (e-mail: tazevedo@utad.pt)*

Abstract: This work focus on gas networks modelling in view to developing leakage detection/location techniques. Concerning leakage detection and its consequences, an economically viable and precise method is required. Using intermediate values of mass-flow and pressure along the pipeline and an electrical analogy, models may be obtained to represent the gas pipeline dynamics. Here we present two port network models based where gas mass flows behave like electrical currents and pressures like voltages. Centered on this analogy we study two cases, (i) one where the pressure depends on gas mass flow, the Impedance case and (ii) other that inversely displays gas mass flow as a function of the pressure, the Admittance case. The relations between parameters and models are also examined and models are validated using real data.

Keywords: Gas networks, Modelling, Dynamic models, Fault detection, Frequency response.

1. INTRODUCTION

The purpose of this work is to improve a model for leakage detection/location in view to the development of model-based (MB) software methods Lopes dos Santos et al. (2011).
MB methods continuously measure the pressure and/or mass-flow signals at different points of the pipeline, mostly only at its extremes. Leakages are detected from the mass-flow balance equations, which consist in balancing the flow at the boundaries plus the variation of linepack in the pipes (i.e., the gas stored within the pipelines) Baptista et al. (2005). However, these methods in dynamic conditions cannot be considered completely reliable since a significant number of false alarm rates is registered Gasodutos (2006). Software methods have the advantage to be less costly to implement. The most reliable among these methods are based on nonlinear partial derivative equations (PDE) that describe the gas dynamics within the pipelines. Still, these PDE models are not modular and lead to non efficient and high complexity methods. In Lopes dos Santos et al. (2010b) it was shown that a PDE linearisation can lead to simple and accurate models. In this paper, we propose a modular model for a non-horizontal gas pipeline Geiger (2006); Verde (2005) based on the PDE linearisation. To assess the importance of the altitude term in the first equation of (1), the behaviour of the proposed model is simulated for different angles of the inclination of the pipeline. A transfer function model is derived for a pipeline by taking advantage of an electrical analogy, where the pipeline is described as quadripole. This allows for ensuring a high degree of modularity that can be used to simulate and detect leaks in complex gas pipeline networks.
This article is organised as follows. In Section 2 the PDE is linearised and in Section 3 the transfer function model is derived. Quadripole models are obtained from the transfer function model in Section 4. In Section 5 the frequency responses of the quadripole models are shown. Conclusions and directions for future work are withdrawn in Section 6.

2. LINEARISED MODEL

Assuming a section of a pipeline whose diameter stays constant and the flow is unidirectional, the gas dynamics in the pipe can be express by a non-linear second order hyperbolic PDE, neglecting the viscous and the turbulent effects of the flow and assuming small temperature changes within the gas as well as small heat exchanges with the surroundings of the pipeline Králik et al. (1988); Osiadacz (1987); Reddy et al. (2006). Hence:

$$\begin{cases} \dfrac{\partial q(\ell,t)}{\partial t} = -\mathcal{A}\dfrac{\partial p(\ell,t)}{\partial \ell} - \dfrac{fc^2}{2\mathcal{D}\mathcal{A}}\dfrac{q^2(\ell,t)}{p(\ell,t)} - \mathcal{A}g\sin\theta\dfrac{p(\ell,t)}{c^2} \\ \dfrac{\partial p(\ell,t)}{\partial t} = -\dfrac{c^2}{\mathcal{A}}\dfrac{\partial q(\ell,t)}{\partial \ell}, \end{cases} \tag{1}$$

where q is the node mass-flow, ℓ is space, t is time, $\mathcal{A}$ is the cross-sectional area, p is the edge pressure-drop, f is the friction factor, c is the isothermal speed of sound, $\mathcal{D}$ is the pipe diameter, g is the acceleration due to gravity, and θ is the angle inclination of the tube.
Both the pressure p and gas mass flow q depend on space and time and therefore we write $p(\ell,t)$ and $q(\ell,t)$.
If we set $p(\ell,t) = P_m + \Delta p(\ell,t)$ and $q(\ell,t) = Q_m + \Delta q(\ell,t)$, where P_m and Q_m are the pressure and gas mass flow operational levels and $\Delta p(\ell,t)$ and $\Delta q(\ell,t)$ are the respective deviations from these values along the pipeline, then neglecting terms of order equal or greater than two we have the following approximation

$$\frac{q^2(\ell,t)}{p(\ell,t)} = \frac{(Q_m + \Delta q(\ell,t))^2}{P_m + \Delta p(\ell,t)} \approx \frac{Q_m^2}{P_m} + 2\frac{Q_m}{P_m}\Delta q(\ell,t) - \\ -\frac{Q_m^2}{P_m^2}\Delta p(\ell,t). \tag{2}$$

Furthermore, the third term of the right side of (2) may be neglected since distribution networks operate at very high pressure, ca. 80 bar. Then use approximation (2) in the first equation of (1) and obtain:

$$\frac{\partial q(\ell,t)}{\partial t} = -\mathcal{A}\frac{\partial p(\ell,t)}{\partial \ell} - \frac{fc^2}{2\mathcal{D}\mathcal{A}}\frac{Q_m}{P_m}(Q_m + 2\Delta q(\ell,t)) - \\ -\mathcal{A}g\sin\theta\frac{p(\ell,t)}{c^2}. \tag{3}$$

Also, assuming small flow oscillations, we may have $Q_m + 2\Delta q(\ell,t) \approx Q_m + \Delta q(\ell,t) = q(\ell,t)$ and thus obtain the following linearised model:

$$\begin{cases} \dfrac{\partial q(\ell,t)}{\partial t} = -\mathcal{A}\dfrac{\partial p(\ell,t)}{\partial \ell} - 2\alpha q(\ell,t) - \beta\sin\theta p(\ell,t) \\ \dfrac{\partial p(\ell,t)}{\partial t} = -\dfrac{c^2}{\mathcal{A}}\dfrac{\partial q(\ell,t)}{\partial \ell}, \end{cases} \tag{4}$$

where

$$\alpha = \frac{fc^2}{4\mathcal{D}\mathcal{A}}\frac{Q_m}{P_m}, \qquad \beta = \frac{\mathcal{A}g}{c^2}. \tag{5}$$

3. TRANSFER FUNCTION MODEL

When applying the Laplace transform to (4), a linear differential equation in ℓ is obtained:

$$\begin{cases} \dfrac{\partial P(\ell,s)}{\partial \ell} = -\dfrac{\beta}{\mathcal{A}}\sin\theta P(\ell,s) - \dfrac{2\alpha+s}{\mathcal{A}}Q(\ell,s) \\ \dfrac{\partial Q(\ell,s)}{\partial \ell} = -s\dfrac{\beta}{g}P(\ell,s). \end{cases} \tag{6}$$

Writing (6) in the matrix form:

$$\begin{bmatrix} \dfrac{\partial P(\ell,s)}{\partial \ell} \\ \dfrac{\partial Q(\ell,s)}{\partial \ell} \end{bmatrix} = \begin{bmatrix} -\dfrac{\beta}{\mathcal{A}}\sin\theta & -\dfrac{2\alpha+s}{\mathcal{A}} \\ -s\dfrac{\mathcal{A}}{c^2} & 0 \end{bmatrix} \begin{bmatrix} P(\ell,s) \\ Q(\ell,s) \end{bmatrix}, \tag{7}$$

where we define

$$X(\ell) = \begin{bmatrix} \dfrac{\partial P(\ell,s)}{\partial \ell} & \dfrac{\partial Q(\ell,s)}{\partial \ell} \end{bmatrix}^T, \tag{8}$$

$$A = \begin{bmatrix} -\dfrac{\beta}{\mathcal{A}}\sin\theta & -\dfrac{2\alpha+s}{\mathcal{A}} \\ -s\dfrac{\mathcal{A}}{c^2} & 0 \end{bmatrix}, \tag{9}$$

$$X(0) = \begin{bmatrix} P(0,s) & Q(0,s) \end{bmatrix}^T. \tag{10}$$

$P(0,s)$ and $Q(0,s)$ are the Laplace transforms of the inlet pressure and mass flow. The solution of (6) is

$$X(\ell) = e^{A\ell}X(0), \tag{11}$$

where $e^{A\ell}$ is the exponential matrix of $A\ell$ and can be written as:

$$e^{A\ell} = \begin{bmatrix} E_{11}(\ell,s) & E_{12}(\ell,s) \\ E_{21}(\ell,s) & E_{22}(\ell,s) \end{bmatrix}, \tag{12}$$

with

$$E_{11}(\ell,s) = \frac{e^{-\delta(s)T_d(\ell)}}{-2\gamma(s)} \cdot \left[\frac{g}{2c}\sin\theta\left(1 - e^{-2\gamma(s)T_d(\ell)}\right) - \gamma(s)\left(1 + e^{-2\gamma(s)T_d(\ell)}\right)\right], \tag{13}$$

$$E_{12}(\ell,s) = \frac{e^{-\delta(s)T_d(\ell)}\left(1 - e^{-2\gamma(s)T_d(\ell)}\right)}{-2\gamma(s)}\frac{c\,(s+2\alpha)}{\mathcal{A}}, \tag{14}$$

$$E_{21}(\ell,s) = \frac{e^{-\delta(s)T_d(\ell)}\left(1 - e^{-2\gamma(s)T_d(\ell)}\right)}{-2\gamma(s)}\frac{s\mathcal{A}}{c} \tag{15}$$

and

$$E_{22}(\ell,s) = \frac{e^{-\delta(s)T_d(\ell)}}{2\gamma(s)} \cdot \left[\frac{g}{2c}\sin\theta\left(1 - e^{-2\gamma(s)T_d(\ell)}\right) + \gamma(s)\left(1 + e^{-2\gamma(s)T_d(\ell)}\right)\right], \tag{16}$$

where

$$T_d(\ell) = \frac{\ell}{c} \tag{17}$$

$$\gamma(s) = \sqrt{(s+\alpha)^2 + \frac{g^2}{4c^2}\sin^2\theta - \alpha^2} \tag{18}$$

$$\delta(s) = \frac{g}{2c}\sin\theta - \gamma(s). \tag{19}$$

Where we observe the relation between the two off-diagonal transfer functions:

$$E_{12}(\ell,s) = \frac{c^2\,(s+2\alpha)}{s\mathcal{A}^2}E_{21}(\ell,s). \tag{20}$$

If we fix $\ell = L$, where L is the pipe length, we obtain $P(L,s)$ and $Q(L,s)$, which are the Laplace transforms of outlet pressure and mass flow. So the solution that relates inlet and outlet pressures and mass flows is:

$$\begin{bmatrix} P(L,s) \\ Q(L,s) \end{bmatrix} = \begin{bmatrix} E_{11}(L,s) & E_{12}(L,s) \\ E_{21}(L,s) & E_{22}(L,s) \end{bmatrix} \begin{bmatrix} P(0,s) \\ Q(0,s) \end{bmatrix} \tag{21}$$

and the pipeline may be described by the following model

$$\begin{cases} P(L,s) = E_{11}(L,s)P(0,s) + E_{12}(L,s)Q(0,s) \\ Q(L,s) = E_{21}(L,s)P(0,s) + E_{22}(L,s)Q(0,s). \end{cases} \tag{22}$$

Notice that $E_{ij}(\ell,s)$, $i,j = 1,2$ are transfer functions

$$E_{ij}(\ell,s) = \left.\frac{\mathcal{Y}_i(s)}{\mathcal{U}_j(s)}\right|_{\mathcal{U}_k=0} \qquad i,j,k = 1,2, \text{ and } k \neq j$$

where the symbol $\mathcal{U}$ stands for input, which in this case means inlet pressure and mass flow, and likewise $\mathcal{Y}$ stands for output, which in this case means outlet pressure and mass flow. The indexes of $\mathcal{U}$ and $\mathcal{Y}$ denote pressure if equal to 1 and massflow if equal to 2.

In the sequel, we drop the argument L in $T_d(L)$ and $E_{ij}(L,s)$, $i,j = 1,2$ and in all transfer functions that may occur.

4. QUADRIPOLE MODELS

Using an analogy between gas pipelines and electrical circuits where gas mass flows behave like electrical currents and pressures behave like voltages we can represent the pipeline dynamics by the quadripole represented in Fig. 1.

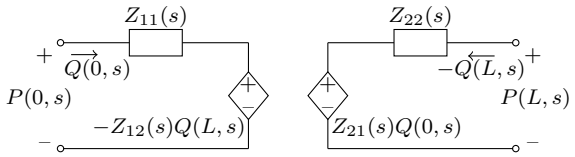

Fig. 1. Gas mass flow independents electrical quadripole.

In this quadripole the voltages $P(0,s)$ and $P(L,s)$ are related with the current sources (independent variables) $Q(0,s)$ and $Q(L,s)$ by the impedance model

$$\begin{cases} P(0,s) = Z_{11}(s)Q(0,s) - Z_{12}(s)Q(L,s) \\ \\ P(L,s) = Z_{21}(s)Q(0,s) - Z_{22}(s)Q(L,s). \end{cases} \tag{23}$$

From here we can see that

$$\begin{aligned} Z_{11}(s) &= \left.\frac{P(0,s)}{Q(0,s)}\right|_{Q(L,s)=0} \quad Z_{12}(s) = \left.\frac{P(0,s)}{-Q(L,s)}\right|_{Q(0,s)=0} \\ Z_{21}(s) &= \left.\frac{P(L,s)}{Q(0,s)}\right|_{Q(L,s)=0} \quad Z_{22}(s) = \left.\frac{P(L,s)}{-Q(L,s)}\right|_{Q(0,s)=0}. \end{aligned}$$

$Z_{i,j}$ can be calculated from (22) taking, successively, $Q(0,s)=0$ and $Q(L,s)=0$:

$$\begin{aligned} Z_{11}(s) &= -\frac{E_{22}(s)}{E_{21}(s)}, & Z_{12}(s) &= -\frac{1}{E_{21}(s)}, \\ Z_{21}(s) &= -\frac{E_{11}(s)E_{22}(s)}{E_{21}(s)} + E_{12}(s), & Z_{22}(s) &= -\frac{E_{11}(s)}{E_{21}(s)}. \end{aligned} \tag{24}$$

Substituting E_{ij}, $1, j = 1,2$ by their values in (13)-(16), these equations can be rewritten as

$$Z_{11}(s) = \frac{c\gamma(s)}{\mathcal{A}s}\frac{1+e^{-2T_d\gamma(s)}}{1-e^{-2T_d\gamma(s)}} + \frac{g}{2\mathcal{A}s}\sin\theta \tag{25}$$

$$Z_{12}(s) = \frac{2ce^{T_d\frac{g}{2c}\sin\theta}\gamma(s)}{\mathcal{A}s}\frac{e^{-T_d\gamma(s)}}{1-e^{-2T_d\gamma(s)}} \tag{26}$$

$$Z_{21}(s) = \frac{2ce^{-T_d\frac{g}{2c}\sin\theta}\gamma(s)}{\mathcal{A}s}\frac{e^{-T_d\gamma(s)}}{1-e^{-2T_d\gamma(s)}} \tag{27}$$

$$Z_{22}(s) = \frac{c\gamma(s)}{\mathcal{A}s}\frac{1+e^{-2T_d\gamma(s)}}{1-e^{-2T_d\gamma(s)}} - \frac{g}{2\mathcal{A}s}\sin\theta. \tag{28}$$

Considering

$$\frac{g^2}{4c^2}\sin^2\theta - \alpha^2 \approx 0 \Leftrightarrow \frac{g^2}{4c^2}\sin^2\theta - \left(\frac{fc^2}{2\mathcal{D}\mathcal{A}}\frac{q_m(L)}{p_m(L)}\right)^2 \approx 0, \tag{29}$$

Z_{ij}, $i,j = 1,2$ may be approximated by

$$\begin{aligned} \hat{Z}_{11}(s) &= K_{11}\left(\frac{s+\alpha}{s}\right)\left(\frac{1+e^{-2T_d(s+\alpha)}}{1-e^{-2T_d(s+\alpha)}}\right) + \frac{g}{2\mathcal{A}s}\sin\theta \\ \hat{Z}_{12}(s) &= K_{12}\left(\frac{s+\alpha}{s}\right)\left(\frac{e^{-T_ds}}{1-e^{-2T_d(s+\alpha)}}\right) \\ \hat{Z}_{21}(s) &= K_{21}\left(\frac{s+\alpha}{s}\right)\left(\frac{e^{-T_ds}}{1-e^{-2T_d(s+\alpha)}}\right) \\ \hat{Z}_{22}(s) &= K_{22}\left(\frac{s+\alpha}{s}\right)\left(\frac{1+e^{-2T_d(s+\alpha)}}{1-e^{-2T_d(s+\alpha)}}\right) - \frac{g}{2\mathcal{A}s}\sin\theta \end{aligned}$$

where K_{ij}, $i,j = 1,2$ are tuned such that

$$\lim_{s\to 0} s\hat{Z}_{ij}(s) = \lim_{s\to 0} sZ_{ij}(s)$$

i.e.,

$$K_{11} = \begin{cases} \dfrac{g}{2\mathcal{A}\alpha}\sin\theta\dfrac{1+e^{-T_d\frac{g}{c}\sin\theta}}{1-e^{-T_d\frac{g}{c}\sin\theta}}\dfrac{1-e^{-2T_d\alpha}}{1+e^{-2T_d\alpha}}, & \theta \neq 0 \\ \dfrac{c}{A\alpha T_d}\dfrac{1-e^{-2T_d\alpha}}{1+e^{-2T_d\alpha}}, & \theta = 0 \end{cases} \tag{30}$$

$$K_{12} = \begin{cases} \dfrac{g}{\mathcal{A}\alpha}\sin\theta\dfrac{1-e^{-2T_d\alpha}}{1-e^{-T_d\frac{g}{c}\sin\theta}}, & \theta \neq 0 \\ \dfrac{c}{A\alpha T_d}\left(1-e^{-2T_d\alpha}\right), & \theta = 0 \end{cases} \tag{31}$$

$$K_{21} = \begin{cases} \dfrac{g}{\mathcal{A}\alpha}e^{-Td\frac{g}{c}\sin\theta}\sin\theta\dfrac{1-e^{-2T_d\alpha}}{1-e^{-Td\frac{g}{c}\sin\theta}}, & \theta \neq 0 \\ \dfrac{c}{A\alpha T_d}\left(1-e^{-2T_d\alpha}\right), & \theta = 0 \end{cases} \tag{32}$$

$$K_{22} = K_{11}. \tag{33}$$

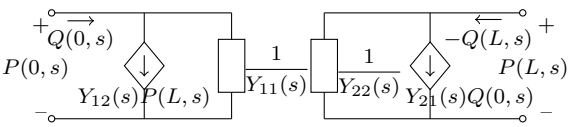

Fig. 2. Gas pressure independents electrical quadripole.

The impedance model (23) takes the inlet and outlet mass flows as independent variables, however, in gas networks operation, the usual situation is to have pressure measurements, since mass flow meters are still expensive or may interfere with the normal operation of the pipelines. As a result, a quadripole model that takes the inlet and outlet pressures as independent variables is more useful. Such quadripole model is portraited in Fig. 2 and is described by the following equations:

$$\begin{cases} Q(0,s) = Y_{11}(s)P(0,s) + Y_{12}(s)P(L,s) \\ \\ Q(L,s) = -Y_{21}(s)P(0,s) - Y_{22}(s)P(L,s), \end{cases} \tag{34}$$

where

$$\begin{aligned} Y_{11}(s) &= \left.\frac{Q(0,s)}{P(0,s)}\right|_{P(L,s)=0} \quad Y_{12}(s) = \left.\frac{Q(0,s)}{P(L,s)}\right|_{P(0,s)=0} \\ Y_{21}(s) &= -\left.\frac{Q(L,s)}{P(0,s)}\right|_{P(L,s)=0} \quad Y_{22}(s) = -\left.\frac{Q(L,s)}{P(L,s)}\right|_{P(0,s)=0}. \end{aligned}$$

From (22)

$$\begin{aligned} Y_{11}(s) &= -\frac{E_{11}(s)}{E_{12}(s)}, & Y_{12}(s) &= \frac{1}{E_{12}(s)}, \\ Y_{21}(s) &= \frac{E_{11}(s)E_{22}(s)}{E_{12}(s)} - E_{21}(s), & Y_{22}(s) &= -\frac{E_{22}(s)}{E_{12}(s)}. \end{aligned} \tag{35}$$

Using relation (20), and the impedance expressions and (25) – (28) we can rewrite the admittances as:

$$Y_{11}(s) = Z_{22}(s)\frac{s\mathcal{A}^2}{c^2\,(s+2\alpha)} = \tag{36}$$
$$= \frac{\mathcal{A}}{c}\frac{\gamma(s)\left(1+e^{-2T_d\gamma(s)}\right)}{(s+2\alpha)\left(1-e^{-2T_d\gamma(s)}\right)} - \frac{g\mathcal{A}}{2c^2\,(s+2\alpha)}\sin\theta$$
$$Y_{12}(s) = -Z_{12}(s)\frac{s\mathcal{A}^2}{c^2\,(s+2\alpha)} = \tag{37}$$
$$= -\frac{2\mathcal{A}e^{T_d\frac{g}{2c}\sin\theta}}{c}\frac{\gamma(s)e^{-T_d\gamma(s)}}{(s+2\alpha)\left(1-e^{-2T_d\gamma(s)}\right)}$$
$$Y_{21}(s) = -Z_{21}(s)\frac{s\mathcal{A}^2}{c^2\,(s+2\alpha)} = \tag{38}$$
$$= -\frac{2\mathcal{A}e^{-T_d\frac{g}{2c}\sin\theta}}{c}\frac{\gamma(s)e^{-T_d\gamma(s)}}{(s+2\alpha)\left(1-e^{-2T_d\gamma(s)}\right)}$$
$$Y_{22}(s) = Z_{11}(s)\frac{s\mathcal{A}^2}{c^2\,(s+2\alpha)} = \tag{39}$$
$$= \frac{\mathcal{A}}{c}\frac{\gamma(s)\left(1+e^{-2T_d\gamma(s)}\right)}{(s+2\alpha)\left(1-e^{-2T_d\gamma(s)}\right)} + \frac{g\mathcal{A}}{2c^2\,(s+2\alpha)}\sin\theta.$$

Using (29), we obtain

$$\hat{Y}_{11}(s) = \bar{K}_{11}\left(\frac{s+\alpha}{s+2\alpha}\right)\left(\frac{1+e^{-2T_d(s+\alpha)}}{1-e^{-2T_d(s+\alpha)}}\right) - \tag{40}$$
$$-\frac{g\mathcal{A}}{2c^2\,(s+2\alpha)}\sin\theta$$
$$\hat{Y}_{12}(s) = -\bar{K}_{12}\left(\frac{s+\alpha}{s+2\alpha}\right)\left(\frac{e^{-T_d s}}{1-e^{-2T_d(s+\alpha)}}\right) \tag{41}$$
$$\hat{Y}_{21}(s) = -\bar{K}_{21}\left(\frac{s+\alpha}{s+2\alpha}\right)\left(\frac{e^{-T_d s}}{1-e^{-2T_d(s+\alpha)}}\right) \tag{42}$$
$$\hat{Y}_{22}(s) = \bar{K}_{22}\left(\frac{s+\alpha}{s+2\alpha}\right)\left(\frac{1+e^{-2T_d(s+\alpha)}}{1-e^{-2T_d(s+\alpha)}}\right) + \tag{43}$$
$$\frac{g\mathcal{A}}{2c^2\,(s+2\alpha)}\sin\theta$$

where $\bar{K}_{ij}$, $i = 1, 2$ are set such that $\hat{Y}_{ij}(0) = Y_{ij}(0)$, i.e.

$$\begin{aligned}\bar{K}_{11} &= \frac{\mathcal{A}^2}{c^2}K_{11},\ \bar{K}_{12} = \frac{\mathcal{A}^2}{c^2}K_{12},\\ \bar{K}_{21} &= \frac{\mathcal{A}^2}{c^2}K_{21},\ \bar{K}_{22} = \bar{K}_{11}.\end{aligned} \tag{44}$$

5. CASE STUDY

To represent the transfer functions, real operational data supplied by REN-Gasodutos were used. Namely:

$$\begin{array}{llll} q_m(L) & = 90\ \text{kg/s} & \text{p}_\text{m}(\text{L}) & = 8\times10^6\ \text{bar} \\ L & = 35580\ \text{m} & \mathcal{A} & = 0,49\ \text{m}^2 \\ f & = 7,9\times10^{-3} & c & = 340\ \text{m/s} \\ \mathcal{D} & = 0,793\ \text{m} & \text{g} & = 9,8\ \text{m/s}^2 \end{array} \tag{45}$$

and we consider three different angles, θ_s; $s = 1, 2, 3$; one that represents a horizontal pipeline $\theta_1 = 0$rad, and two others, $\theta_2 = \pi/12$rad, and $\theta_3 = -\pi/12$rad, that represent an angle between the horizontal and the pipeline.

The influence of the $\theta_s; s = 1, 2, 3$; values is not negligible as shown in Fig. 3 and Fig. 4 where the Bode diagrams of

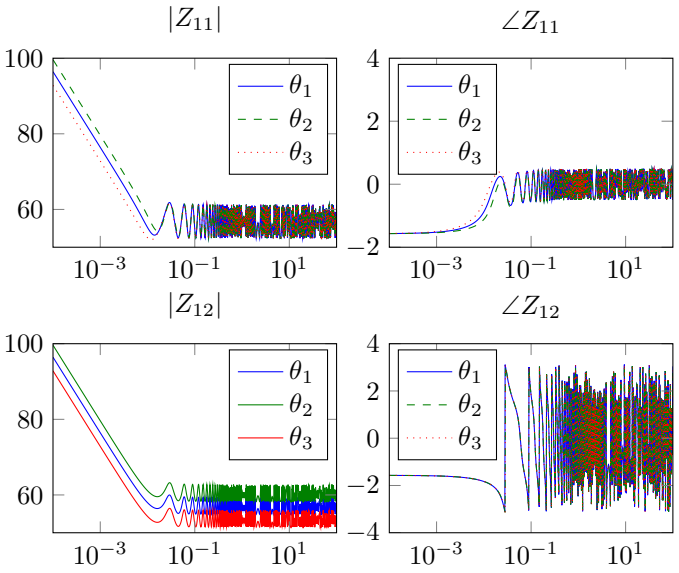

Fig. 3. Bode diagrams of $|Z_{11}|$, $\angle Z_{11}$ and $|Z_{12}|$, $\angle Z_{12}$, for $\theta_1 = 0$ rad, $\theta_2 = \pi/12$ rad and $\theta_3 = -\pi/12$ rad.

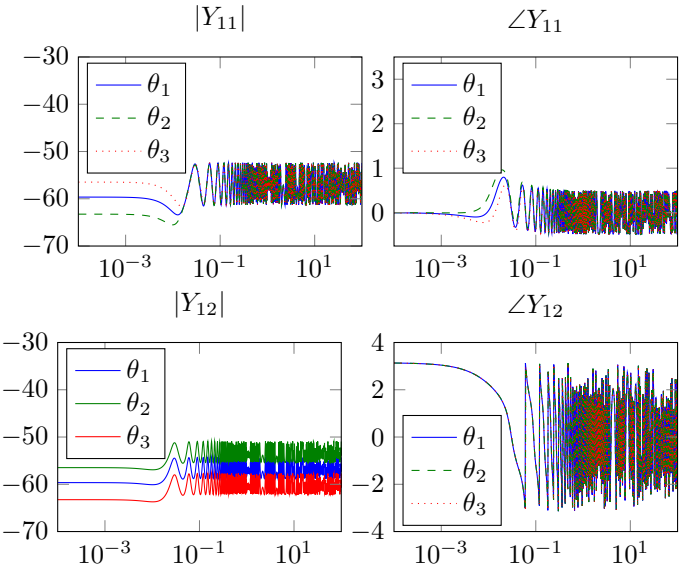

Fig. 4. Bode diagrams of $|Y_{11}|$, $\angle Y_{11}$ and $|Y_{12}|$, $\angle Y_{12}$, for $\theta_1 = 0$ rad, $\theta_2 = \pi/12$ rad and $\theta_3 = -\pi/12$ rad.

Z_{ij} and Y_{ij} are compared for these θ_s.

Next, we analyse the behaviour of $\widehat{Z}_{11}$, $\widehat{Z}_{12}$, $\widehat{Y}_{11}$, and $\widehat{Y}_{12}$ for the three θ_s : To do this, we show the Bode diagrams of these approximated transfer functions for the three different angles in Fig. 5, Fig. 6, Fig. 7, and Fig. 8, respectively.

The impedance model (24) with the approximated transfer functions $\hat{Z}$ and $\theta_1 = 0$ was simulated taking two normal days operation data as the inlet and outlet massflows. Figures 9 and 10 compare the inlet and outlet pressure values with the ones simulated with SIMONE®, one of the standard gas network simulators in the industry. In both cases, the model has well captured the dynamics of the system and, therefore, it seems to be a valuable tool for

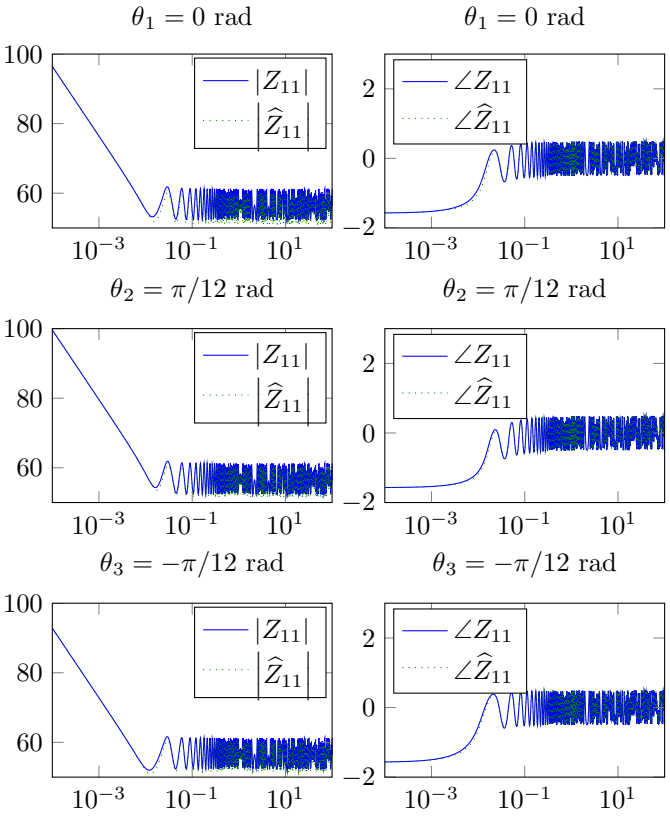

Fig. 5. Bode diagrams of $|Z_{11}|$, $\angle Z_{11}$ and $\left|\widehat{Z}_{11}\right|$, $\angle \widehat{Z}_{11}$, for $\theta_1 = 0$ rad, $\theta_2 = \pi/12$ rad and $\theta_3 = -\pi/12$ rad.

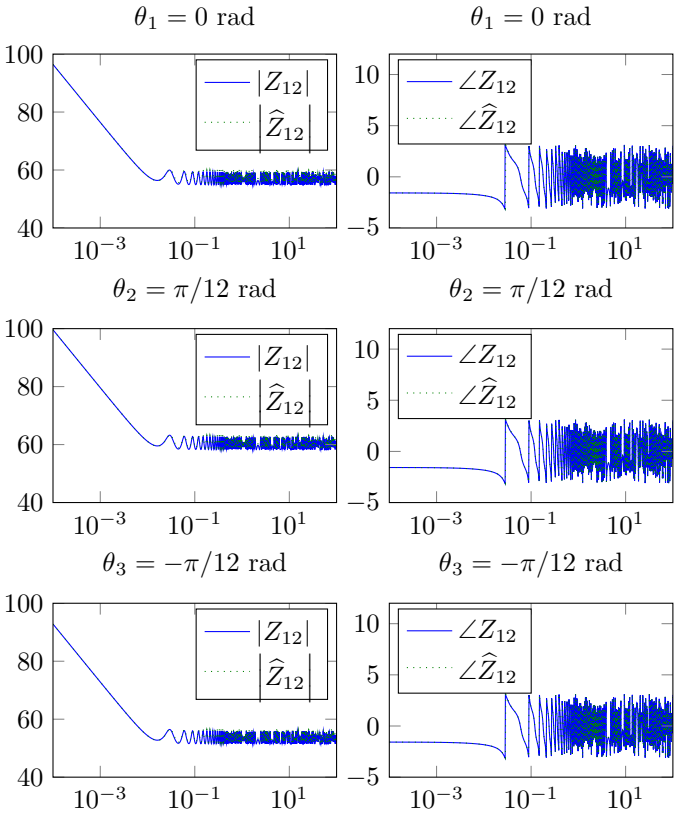

Fig. 6. Bode diagrams of $|Z_{12}|$, $\angle Z_{12}$ and $\left|\widehat{Z}_{12}\right|$, $\angle \widehat{Z}_{12}$, for $\theta_1 = 0$ rad, $\theta_2 = \pi/12$ rad and $\theta_3 = -\pi/12$ rad.

gas leakage detection and gas networks controller design.

6. CONCLUSION

Quadripole TF models were derived for high pressure natural gas pipelines. The nonlinear PDE model describing the pipeline dynamics was linearised, then a TF model was obtained by solving the spatial linear differential equation. Using an electrical analogy modular quadripole models were obtained relating the pressures and massflows in the pipeline boundaries. The transfer functions in the quadripole models were approximated by simpler functions. In a real case study it was shown that the angle inclination of the pipeline has a significant influence on the gas dynamics. The simulated values of the approximated model using two normal days operation data were close to the ones simulated by the SIMONE® simulator.

REFERENCES

Baptista, H., Wagner, G., and Bernhard, W. (2005). Hydraulic model based gas leak detection and location. In *7th Global Congress on Information and Communication Technology in Energy*.

Gasodutos, R. (2006). Personal communication.

Geiger, G. (2006). State-of-the-Art in Leak Detection and Localisation. In *Pipeline Technology 2006 Conference*, 25. Hannover, German.

Králik, J., Stiegler, P., Vostrý, Z., and Závorka, J. (1988). *Dynamic Modeling of Large-Scale Networks with Application to Gas Distribution*. Elsevier, Prague, Czechoslovakia.

Lopes dos Santos, P., Azevedo-Perdicoúlis, T.P., Ramos, J.A., Martins de Carvalho, J.L., Jank, G., and Milhinhos, J. (2010a). Modelling a Leakage in a High Pressure Gas network using a quadripole approach. In *10th Simone Congress*. Constance, Germany.

Lopes dos Santos, P., Azevedo-Perdicoúlis, T.P., Jank, G., Ramos, J.A., and Martins de Carvalho, J.L. (2010b). A lumped transfer function model for high pressure gas pipelines. In *Proceedings of the CDC 2010*. Atlanta, EUA.

Lopes dos Santos, P., Azevedo-Perdicoúlis, T.P., Ramos, J.A., Martins de Carvalho, J.L., Jank, G., and Milhinhos, J. (2011). An LPV Modeling and Identification Approach to Leakage Detection in High Pressure Natural Gas Transportation Networks. In *IEE Transactions on Control Systems Technology*, volume 19, 77–92.

Lopes dos Santos, P., de Azevedo Perdicoúlis, T.P., Ramos, J.A., Jank, G., and Martins de Carvalho, J.L. (2010c). Transportation gas pipelines, Transfer function models. *submitted to Computational and Applied Mathematics*.

Osiadacz, A.J. (1987). *Simulation and Analysis of Gas Networks*. E. & F.N. Spon, London.

Reddy, H.P., Narasimhan, S., and Bhallamudi, S.M. (2006). Simulation and State Estimation of Transient Flow in Gas Pipeline Networks Using a Transfer Function Model. *Industrial & Engineering Chemistry Research*, 45, 3853–3863.

Verde, C. (2005). Accommodation of multi-leak location in a pipeline. *Control Engineering Practice*, 13(8), 1071–

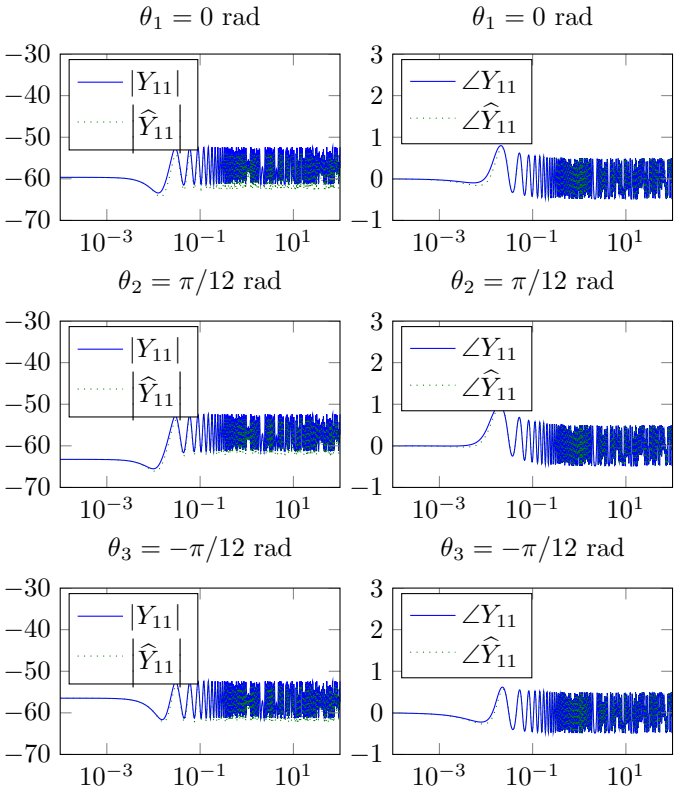

Fig. 7. Bode diagrams of $|Y_{11}|$, $\angle Y_{11}$ and $\left|\widehat{Y}_{11}\right|$, $\angle \widehat{Y}_{11}$, for $\theta_1 = 0$ rad, $\theta_2 = \pi/12$ rad and $\theta_3 = -\pi/12$ rad.

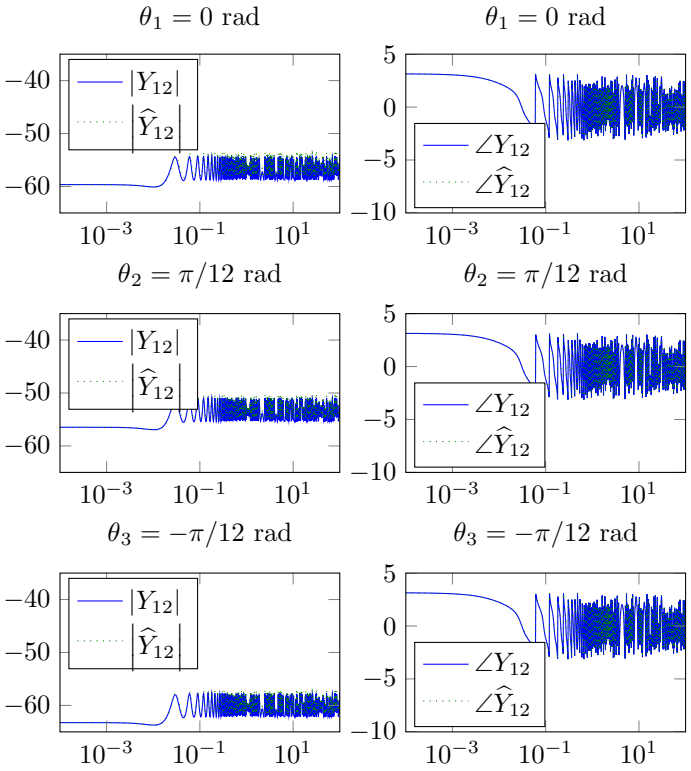

Fig. 8. Bode diagrams of $|Y_{12}|$, $\angle Y_{12}$ and $\left|\widehat{Y}_{12}\right|$, $\angle \widehat{Y}_{12}$, for $\theta_1 = 0$ rad, $\theta_2 = \pi/12$ rad and $\theta_3 = -\pi/12$ rad.

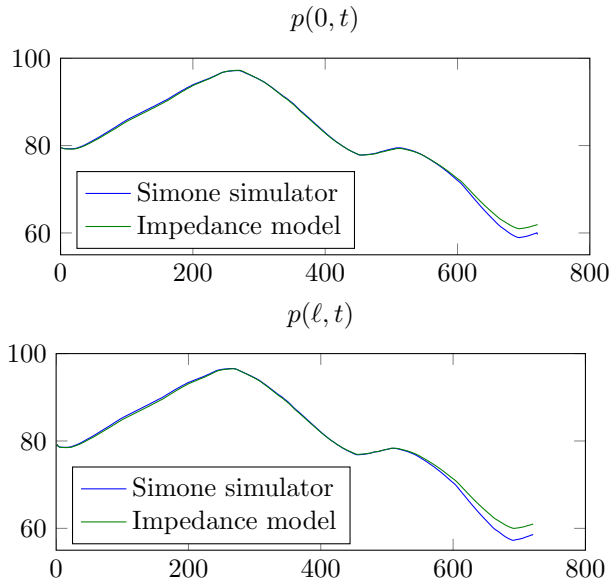

Fig. 9. Input and output pressures $p(0,t)$ and $p(\ell,t)$, respectively, for $\theta_1 = 0$ rad, using first day data.

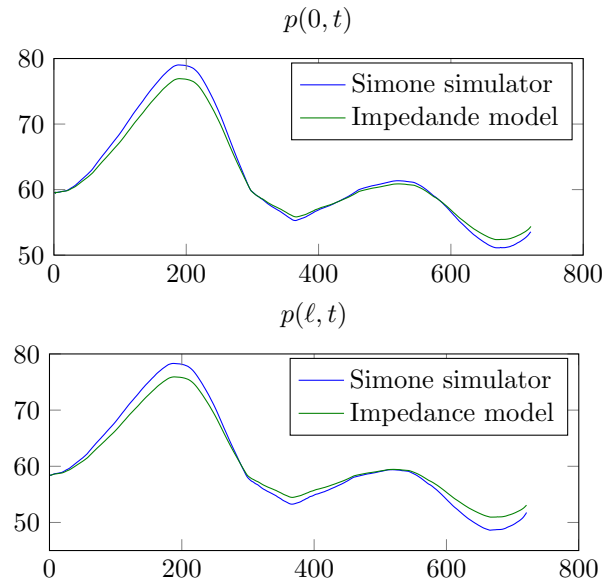

Fig. 10. Input and output pressures $p(0,t)$ and $p(\ell,t)$, respectively, for $\theta_1 = 0$ rad, using second day data.

1078.